J Mater Sci (2015) 50:5238–5243
DOI 10.1007/s10853-015-9071-4

Metastable microstructures containing zero valent iron for fast degradation of azo dyes

F. Scaglione[1] · L. Battezzati[1]

Received: 12 January 2015 / Accepted: 28 April 2015 / Published online: 6 May 2015

Abstract A novel iron powder obtained by ball milling ribbons of a rapidly solidified cast iron was tested for azo dye degradation in aqueous solution versus commercial Fe and a Fe-based metallic glass powders. The cast iron powders were at least as efficient in promoting the degradation reaction of ethyl-orange and direct blue-6 as the ball-milled metallic glass: dyes decomposition was complete in about an hour. The efficiency of alloy samples increases as a function of the decrease of particles size and does not appear to be strongly due to the structure of the phase containing Fe. The main reason for catalytic efficiency is the presence of metastable phases in the material. The zero valent iron that they contain is more prone to provide electrons for the degradation of N–N double bonds. The starting material is cheap and the sample preparation is straightforward. Therefore, it is believed these samples are suitable for fast degradation at room temperature of azo dyes compared with metallic glasses recently proposed in the literature.

Introduction

Zero valent metals are suggested for use in decomposition of organic molecules commonly employed in several industrial applications which cause waste water pollution [1–3]. The most common material employed so far is zero valent iron (ZVI), commercially available in the form of a metal powder, displaying good efficiency although limited durability due to its corrosion tendency. Various reports appeared recently have shown that the decomposition of azo dyes can be substantially accelerated by employing iron in other forms, specifically powders of a Fe-based metallic glass either atomized or obtained by ball milling glassy ribbons [4]. The latter material proved much more efficient than the former, indicating that the rough and kinked surface of ball-milled powders offers very likely much more active sites than the smooth surface of atomized droplets of the same composition. Both materials decompose azo dyes faster than commercially pure Fe powders. On one hand, this is surprising since the Fe content of the metallic glasses is typically of the order of 80 at.%; therefore, it is expected that the number of surface active sites be lower than that of pure Fe; on the other hand, the structural state of Fe atoms in the metastable amorphous alloy differs markedly from that of crystalline Fe. This was suggested as a reason for improved activity of surface Fe atoms. It is in any case difficult to quantify the actual active surface area, and the consequent the Fe content of the surface of these powders, since the size of the particles is of the order of microns if not tens of microns. There is still then uncertainty on the reason for improved efficiency.

With this scenario in mind, we have devised two types of experiments. At first, the catalytic activity of ZVI was tested for Fe-based materials of different compositions and structures using bulk samples having macroscopically the same surface area aiming at ranking their efficiency. Then, the decomposition of dyes was attempted using fine powders obtained by ball milling of the more efficient ones. The materials chosen are a cube of iron having an edge of 1 cm, a $Fe_{82}Si_{13}B_9$ amorphous foil, and a cast iron foil

✉ F. Scaglione
federico.scaglione@unito.it

[1] Dipartimento di Chimica e Centro NIS, Università di Torino, V. Giuria 7, 10125 Turin, Italy

equally obtained by rapid solidification (RS). The reason for employing the RS cast iron is that it has a fine microstructure made of ferrite and cementite with some amount of retained austenite, i.e. it contains metastable crystalline phases, and, in addition, it is definitely cheaper than the metallic glass.

Experimental

Materials and methods

Chemical grade azo dyes, direct blue 6 ($C_{32}H_{20}N_6Na_4O_{14}S_4$) and ethyl-orange ($C_{16}H_{18}N_3NaO_3S$), and distilled water (Elix Millipore, resistivity 5.4 MΩ cm^{-1} @ 25 °C) have been used to prepare aqueous solution with concentration of 0.2 g l^{-1}. For each degradation experiment, the ratio of grams of samples to volume of solution was kept constant at 13.4 g l^{-1} for a comparison with other works in the literature [4]. Experiments have been collected in duplicates to check reproducibility.

Cubes having edge of 1 cm were machined from a sheet of mild steel and polished on all sides as for conventional metallography. Fe powder (99.9 % grade) was from Strem Chemicals, Newburyport, MA, USA (product n. 7439-89-6). Cast iron ribbons and powders were prepared as detailed in the next section. A commercial foil of Metglas® 2605SA1 [5], a magnetic material employed in the core of distribution transformers of approximate composition $Fe_{82}Si_9B_{13}$, was purchased and cut in pieces of size comparable with those of the cast iron ribbons. Ribbons and powders have been characterized by X-ray diffraction (XRD) in Bragg–Brentano geometry with monochromatic Co Kα radiation and scanning electron microscopy (SEM).

The cubes, ribbons, or powders were introduced in a test tube together with the dye solution and kept at room temperature without stirring the solution. Portions of 1 ml of solution were pipetted out, diluted appropriately, and filtered to measure the ultraviolet–visible (UV) absorption spectrum as a function of reaction time.

Fourier transform infrared spectra (FTIR) of the azo dye and of the degraded insoluble products were obtained with a FTIR Bruker IFS 28 averaging 64 scans for each measurement. Degradation products were separated from the powder by dissolving them in ethanol. The solution was then pipetted out after powder settling. After ethanol gets evaporated completely, the product residue was recovered as a powder which was prepared for FTIR by mixing 10 % (w/w) of specimen with KBr and pressing into a thin pellet. The control azo dye spectrum was collected in attenuated total reflectance (ATR), pressing the pure compound onto a diamond window. ATR measurement is corrected for a direct comparison of the two spectra.

Manufacture of cast iron samples

Lumps of a cast iron ingot of industrial production having Carbon equivalent of 4.31 % i.e. 3.72 wt% C and 1.78 wt% Si, ($Fe_{82}C_{15}Si_3$ in at.%) have been induction melted and rapidly solidified by means of a melt spinning apparatus in the form of ribbons about 25-μm thick and 1-cm wide. An Ar protective atmosphere was employed during the RS processing [6]. This resulted in a white cast iron whose microstructure is made of equiaxed crystals of ferrite and cementite on the side which was in contact with the spinning wheel (Fig. 1). The crystals then become dendritic in the central part of the ribbon up to the external side. They are some hundreds of nanometer in thickness and several micrometres long with short lateral arms around a micron in size. The phase constitution is made of ferrite, cementite, i.e. the expected eutectic mixture, and retained austenite as indicated by XRD patterns taken on both sides of the ribbons (Fig. 2). Here, the reflections have varied intensity because of the oriented dendrites seen in Fig. 1. The austenite is metastable at low temperature and transforms into ferrite and cementite on heating above 400 °C [6]. The cementite is obviously metastable in the Fe–C system, but the microstructure obtained by RS has a further degree of metastability in that the ferrite is slightly super saturated in C and the cementite off-stoichiometric [7]. Despite containing some austenite, the ribbons are brittle. Therefore, portions of them have been ball-milled for 8 or 24 h in an agate cell to get powders of different sizes.

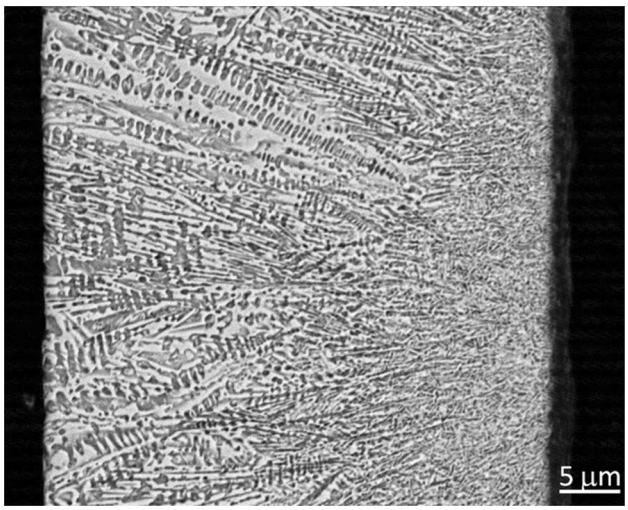

Fig. 1 SEM image of a cross section of a cast iron ribbon produced by rapidly solidification (wheel side on the right)

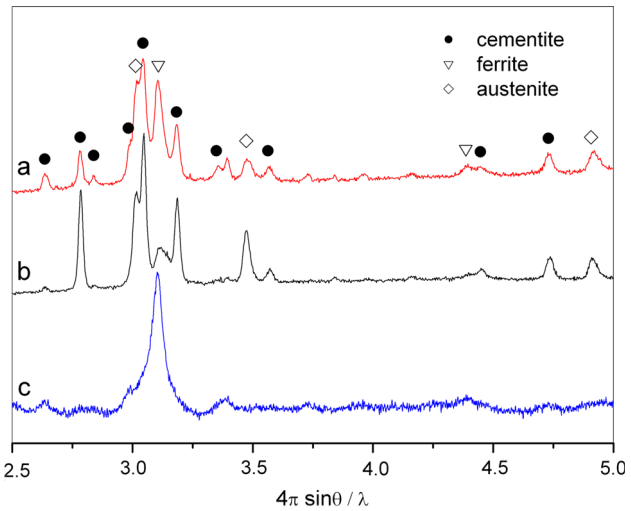

Fig. 2 XRD patterns of the wheel (*a*) and external (*b*) sides of a cast iron ribbon produced by rapidly solidification, (*c*) after ball milling for 24 h

Results and discussion

Degradation of dyes is reported and discussed sequentially on bulk samples and ball-milled cast iron.

Bulk samples

Samples of different structures and compositions but having the same geometrical external area are all active for dye degradation as shown in Fig. 3. We confirm the finding in [4, 8] that amorphous alloys, here $Fe_{82}Si_9B_{13}$, degrade the dye faster than iron. The RS cast iron appears on average as good as the metallic glass in view also of being produced with the same melt spinning technique; therefore, the surfaces of the two materials are well comparable. It is well known, in fact, that melt spun ribbons display a dull surface, the one in contact with the spinning wheel, and a shiny surface, the opposite one. The difference is caused by asperities of the wheel, which are replicated in the ribbon and by bubbles of protective gas entrapped between wheel and ribbon. Both RS materials have the same Fe content of 82 at.% but different structures; therefore, their activities should be due to a cause diverse from geometry of sample, composition, and structural state.

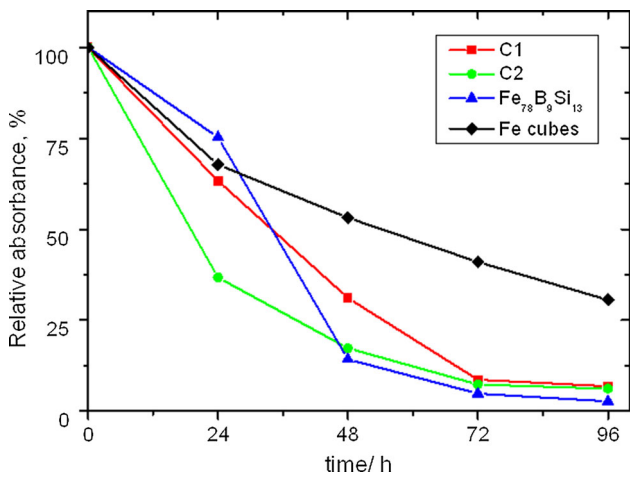

Fig. 3 Normalized UV–visible absorption as a function of treatment time for bulk samples: C1 and C2 were white cast iron ribbons of the same composition, $Fe_{82}Si_9B_{13}$ was a glassy foil, and Fe was in the form of polished cubes. All samples had the same geometrical external area. Experiments of ethyl-orange degradation were performed at room temperature

Ball-milled cast iron

For any application, a high surface area is required and therefore the ribbons must be processed to obtain powders of fine grains. In [4], it was shown that ball-milled powders of an amorphous alloy are much more preferable than atomized powders, very likely because they are made of irregular, instead of smooth, rounded particles. The higher surface area was attributed to complex fracture surfaces. Analogously, cast iron powders were than made by ball milling the ribbons.

After ball milling for 8 h, the ribbons are fragmented in fine pieces which, however, still retain mostly a plate-like shape (see inset of Fig. 4). The aspect ratio of the platelets is of the order of 10. The absorbance of the ethyl-orange solution in contact with the BM-powder is shown in Fig. 4a: it decreases steadily with time and practically vanishes after 26 h as shown by the trend of the maximum of the absorbance in Fig. 4b. Since the phase constitution of the material was not changed during the ball milling process as shown by the invariance of the angular position and number of reflections in XRD patterns of the powders with respect to those reported in Fig. 2, the acceleration of dye degradation must be entirely attributed to the increased amount of active surface available for the reaction. After ball milling for 24 h, the aspect ratio of the particles was reduced by a factor of ten and their shape became roundish (inset in Fig. 5). Still the phases in the powders remained as in the original ribbon, but broadening of reflections due to the reduced size of scattering domains and loss of orientations have been observed especially for the more brittle phase, cementite (Fig. 2) which is known to finely subdivide and eventually dissolve in ferrite as a consequence of heavy deformation [9, 10]. Their efficiency in degrading the dyes rapidly is demonstrated by the spectra in Fig. 5a. The trend of the maximum of absorbance (both ethyl-orange and direct blue-6) as a function of time is in given Fig. 5b. The de-colouring is complete in less than 1 h, a time well comparable with that of ball-milled amorphous

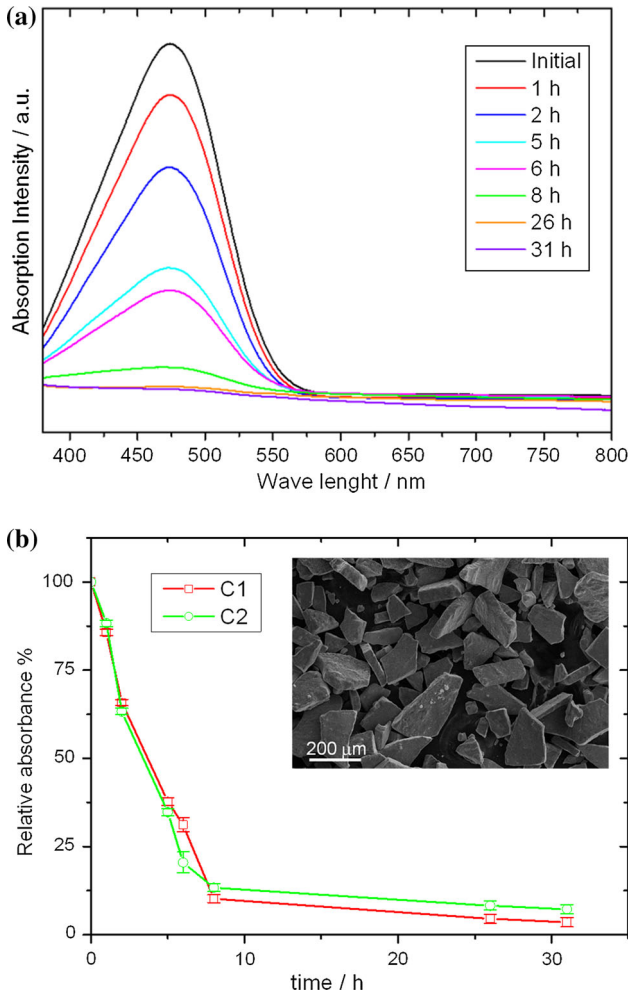

Fig. 4 **a** UV–visible absorption of ethyl-orange solutions as a function of residence time on C1 and C2 white cast iron powders obtained by ball milling ribbon portions for 8 h. **b** The maximum of the absorbance as a function of residence time. The *inset* is the SEM image of the powder showing a *plate-like shape*

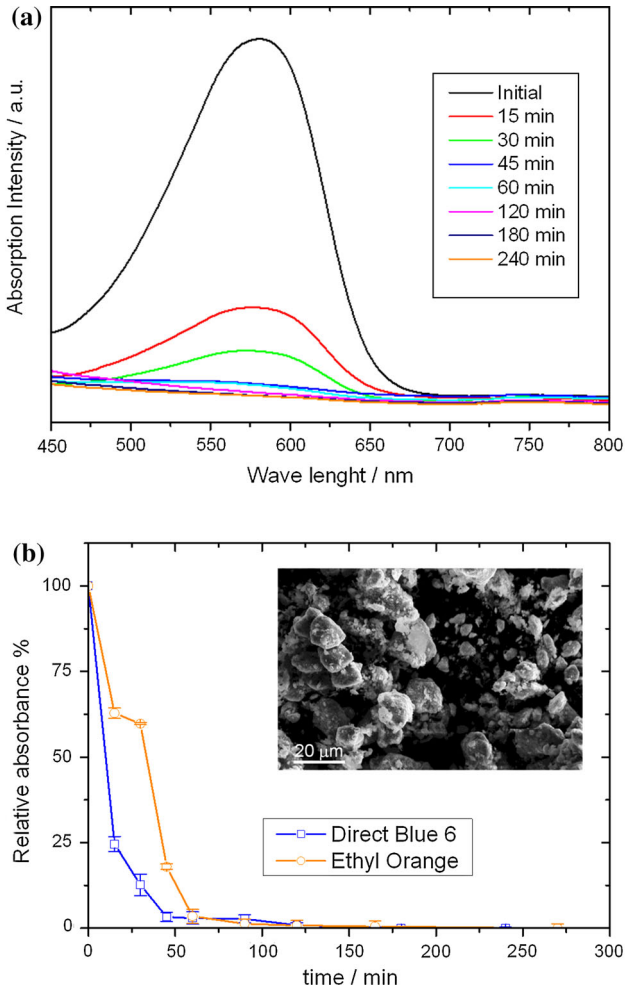

Fig. 5 **a** UV–visible absorption of direct blue-6 solutions as a function of residence time on C1 and C2 white cast iron powder obtained by ball milling ribbon portions for 24 h. **b** The maximum of the absorbance as a function of residence time for both ethyl-orange and direct blue-6. The *inset* is the SEM image of the powder displaying *roundish shape*

ribbons reported earlier with curves compatible with a first-order exponential decay as well [4]. For countercheck, we performed also the degradation of dyes by means of commercial Fe powders, 1–5 µm in size: it was much slower in that the absorbance was halved in about 50 h confirming previous results [4]. After being dispersed in the solution, the particles tend to aggregate being all ferromagnetic [11, 12]; moreover, with the advancement of degradation, non-soluble decomposition products sedimented together with the powders. However, the efficiency of powders is not hindered; indeed if a new portion of solution is added to the powder already used, without washing the sediment out, a second degradation cycle is possible with the same kinetics, i.e. no apparent passivation. Up to four consecutive degradation cycles, the kinetics is only slightly slowed of 5 and 7 %, respectively, for the third and fourth cycle. This indicates the efficiency is maintained as long as Fe atoms in active sites are prone to oxidize to Fe^{2+}. In fact, the reduction mechanism of azo dyes is basically due to a redox reaction between Fe atoms and –(N=N)– azo dye bonds [8], splitting the dye in aromatic amine [13] and other compounds such as aniline [14]. FTIR spectra of degraded products have been collected in the range of 500–4000 cm^{-1} and compared with that of the dye before treatment. In Fig. 6, the bands of spectrum (a) are associated respectively: peaks at 640 and 977 cm^{-1} are attributed to S=O and C–O stretching, at 1044, 1186, and 1340 cm^{-1} to asymmetric and symmetric stretching of C–N, at 1492 and 3421 cm^{-1} to symmetric stretching of N–H, and at 1615 and 2924 cm^{-1} to stretching of –N=N– and C–H [15]. In spectrum (b), the stretching of –N=N– disappears, while new peaks

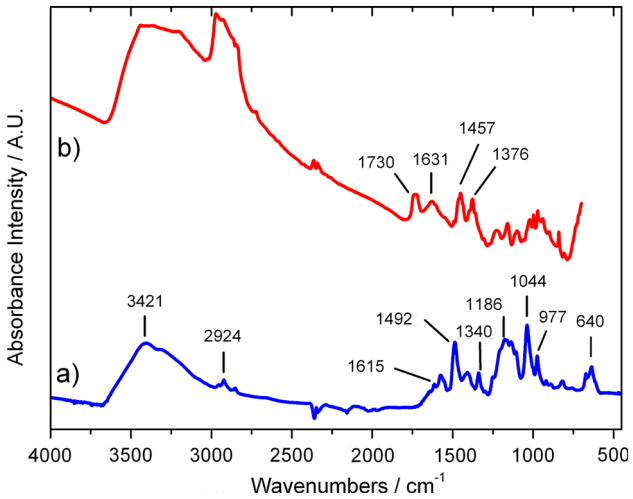

Fig. 6 FTIR spectra of **a** direct blue 6 azo dye and **b** degraded products after treatment with C1 and C2 white cast iron powder obtained by ball milling portions of a ribbon for 24 h

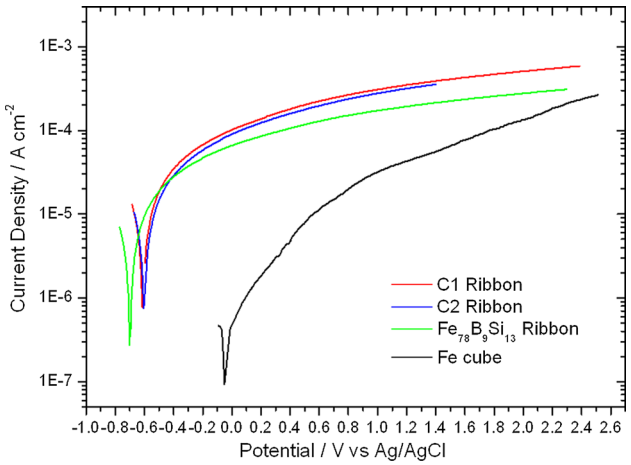

Fig. 7 Potentiodynamic polarization curves in 0.2 g l^{-1} ethyl-orange azo-dye solution for samples listed in the legend. Experiments were performed at room temperature with a scan rate of 20 mV s^{-1}

associated to degraded products of the dye appear: peaks at 1631,1730, and 1376 cm^{-1}, respectively, are attributed to scissor vibration of N–H and C–N vibration in aromatic amines, and at 1457 cm^{-1} to the C=C stretching vibration of the aromatic ring [16]. This confirms literature results showing that the breaking of the chromophore bond could probably form anilines and benzenesulfonic acids [17]. It is reckoned that adsorption of dyes occurs on the iron prior to degradation. However, this does not cause passivation of powders up to at least four degradation cycles. The catalyzer was found to become exhausted due to formation of iron oxides identified in XRD patterns. At this stage, adsorption phenomena could still give rise to some decoloring since the high adsorption properties of iron oxides particles have been recently proven [18].

In summary, both the as-cast ribbons of cast iron and the ball-milled powders obtained with them are at least as active towards dye degradation as Fe-based amorphous alloys, being certainly much cheaper. On a more fundamental ground, the results obtained in this work show that the structure of the material does not appear to be the determining factor for its catalytic activity. Since the commercially pure Fe is in any case less active, it is suggested that the occurrence of metastable phases is most relevant being these more prone to provide electrons to break the N–N bonds of the dyes according to the reaction mechanism outlined in [19, 20]. To this respect, we recorded both the open circuit voltage (OCV) and potentiodynamic behaviour of ribbons of cast iron and glassy $Fe_{82}Si_9B_{13}$. The OCV is about 0.5 and 0.65 V, respectively, and the corrosion potential is 0.6 and 0.7 V more negative (Fig. 7) with respect to those of a Fe foil. It is concluded that the catalytic effect on azo dye degradation stems from the increased electrochemical activity of the material. It is worth noting that an even faster reaction rate was recently reported for Mg–Zn–Ca metallic glasses [21], i.e. a more corrodible alloy, although definitely more expensive than cast iron. Finally, we note that the corrosion products of white cast iron are well known and dealt with in water remediation, i.e. Fe oxides, hydrocarbons, or carbonates according to the pH of the solution and the eventual applied potential [22, 23]. The rapidly solidified and ball-milled cast iron looks than more advantageous in dye degradation than other forms of ZVI tested in this work, namely commercial pure Fe and a metallic glass.

Conclusion

The present work shows that powders made by ball milling ribbons of rapidly solidified cast iron, a white cast iron containing ferrite, cementite, and retained austenite, are good catalytic materials for the degradation of organic dyes. RS is essential to obtain the above phase mixture and a fine size of crystals. The ribbons are brittle and, therefore, suited for ball milling which should be prolonged enough to reduce the particle aspect ratio to about one (24 h with the working procedure used here) while keeping the phase constitution of the material unchanged. The cast iron powders are as effective as the best Fe-based materials proposed to date in the literature (i.e. ball-milled amorphous alloys), although definitely cheaper, for the degradation of dyes. The increased reactivity proven also by electrochemical analyses will certainly also enhance the corrosion rate of the alloy powders since the oxidation of Fe is inherent to the process. Using this material will then be a matter of trade-off between the need for fast

degradation and that for powder replacement although clear advantages are recognized, i.e. large availability and low price, and fast degradation kinetics.

Acknowledgements The Authors acknowledge the financial support from "Progetto di Ateneo a valere su Convenzione Intesa San-Paolo, *Advances in nanostructured materials and interfaces for key technologies*".

References

1. Zhang WX (2003) Nanoscale iron particles for environmental remediation: an overview. J Nanopart Res 5:323–332
2. Arnold WA, Roberts AL (1998) Pathways of chlorinated ethylene and chlorinated acetylene reaction with Zn(0). Environ Sci Technol 32:3017–3025
3. Fennelly JP, Roberts AL (1998) Reaction of 1,1,1-trichloroethane with zero-valent metals and bimetallic reductants. Environ Sci Technol 32:1980–1988
4. Wang JQ, Liu YH, Chen MW, Xie GQ et al (2012) Rapid degradation of azo dye by Fe-based metallic glass powder. Adv Funct Mater 22:2567–2570
5. Metglass, Inc., 2605SA1 alloy, Technical Bulletin
6. Battezzati L, Baldi P, Baricco M, Bosco E, Goria CA, Serramoglia G, Marongiu F (2003) Solidification experiments for the study of phase selection in cast iron. Int J Cast Metal Res 16:125–129
7. Battezzati L, Baricco M, Curiotto S (2005) Non-stoichiometric cementite by rapid solidification of cast iron. Acta Mater 53:1849–1856
8. Zhang CQ, Zhang HF, Lv MQ, Hu ZQ (2010) Decolorization of azo dye solution by Fe–Mo–Si–B amorphous alloy. J Non Cryst Solids 356:1703–1706
9. Liu ZG, Fechta HJ, Umemoto M (2004) Microstructural evolution and nanocrystal formation during deformation of Fe–C alloys. Mater Sci Eng A 375–377:839–843
10. Umemoto M, Liu ZG, Masuyama K, Hao XJ, Tsuchiya K (2001) Nanostructured Fe–C alloys produced by ball milling. Scr Mater 44:1741–1745
11. Fan J, Guoa Y, Wanga J, Fan M (2009) Rapid decolorization of azo dye methyl orange in aqueous solution by nanoscale zerovalent iron particles. J Hazard Mater 166:904–910
12. He F, Zhao D (2005) Preparation and characterization of a new class of starch-stabilized bimetallic nanoparticles for degradation of chlorinated hydrocarbons in water. Environ Sci Technol 39:3314–3320
13. Pielesz A, Baranowska I, Rybak A, Wlochowicz A (2002) Detection and determination of aromatic amines as products of reductive splitting from selected azo dyes. Ecotoxicol Environ Saf 53:42–47
14. Samarghandi MR et al (2012) Kinetic of degradation of two azo dyes from aqueous solutions by zero iron powder: determination of the optimal conditions. Desalination Water Treat 40:137–143
15. Kalme S, Jadhavb S, Jadhavb M, Govindwara S (2009) Textile dye degrading laccase from Pseudomonas desmolyticum NCIM 2112. Enzyme Microb Technol 44:65–71
16. Socrates G (2004) Infrared and Raman characteristic group frequencies: tables and charts, 3rd edn. Wiley, Hoboken
17. Li P, Song Y, Wang S, Tao Z, Yu S, Liu Y (2015) Enhanced decolorization of methyl orange using zero-valent copper nanoparticles under assistance of hydrodynamic cavitation. Ultrason Sonochem 22:132–138
18. Jia Z, Liu J, Wang Q, Li S, Qi Q, Zhu R (2015) Synthesis of 3D hierarchical porous iron oxides for adsorption of Congo red from dye wastewater. J Alloy Compd 622:587–595
19. Agrawal A, Tratnyek PG (1996) Reduction of nitro aromatic compounds by zero-valent iron metal. Environ Sci Technol 30:153–160
20. Cao J, Wie L, Huang Q, Wang L, Han S (1999) Reducing degradation of azo dye by zero-valent iron in aqueous solution. Chemosphere 38:565–571
21. Wang JQ, Liu YH, Chen MW et al (2012) Excellent capability in degrading azo dyes by MgZn-based metallic glass powders. Sci Rep. doi:10.1038/srep00418
22. Pascal P et al (1967) Nouveau Traité de Chimie Minérale, Tome XVII. Masson et Cie, Paris
23. Bouzek K, Bergmann H (1999) Comparison of pure and white cast iron dissolution kinetics in highly alkaline electrolyte. Corros Sci 41:2113–2128